Article

# Tail-propelled aquatic locomotion in a theropod dinosaur

https://doi.org/10.1038/s41586-020-2190-3

Received: 17 June 2019

Accepted: 19 February 2020

Published online: 29 April 2020

Check for updates

Nizar Ibrahim[1]✉, Simone Maganuco[2,3], Cristiano Dal Sasso[3], Matteo Fabbri[4], Marco Auditore[3], Gabriele Bindellini[3,5], David M. Martill[6], Samir Zouhri[7], Diego A. Mattarelli[3], David M. Unwin[8], Jasmina Wiemann[4], Davide Bonadonna[2], Ayoub Amane[7], Juliana Jakubczak[1], Ulrich Joger[9], George V. Lauder[10] & Stephanie E. Pierce[10]✉

In recent decades, intensive research on non-avian dinosaurs has strongly suggested that these animals were restricted to terrestrial environments[1]. Historical proposals that some groups, such as sauropods and hadrosaurs, lived in aquatic environments[2,3] were abandoned decades ago[4–6]. It has recently been argued that at least some of the spinosaurids—an unusual group of large-bodied theropods of the Cretaceous era—were semi-aquatic[7,8], but this idea has been challenged on anatomical, biomechanical and taphonomic grounds, and remains controversial[9–11]. Here we present unambiguous evidence for an aquatic propulsive structure in a dinosaur, the giant theropod *Spinosaurus aegyptiacus*[7,12]. This dinosaur has a tail with an unexpected and unique shape that consists of extremely tall neural spines and elongate chevrons, which forms a large, flexible fin-like organ capable of extensive lateral excursion. Using a robotic flapping apparatus to measure undulatory forces in physical models of different tail shapes, we show that the tail shape of *Spinosaurus* produces greater thrust and efficiency in water than the tail shapes of terrestrial dinosaurs and that these measures of performance are more comparable to those of extant aquatic vertebrates that use vertically expanded tails to generate forward propulsion while swimming. These results are consistent with the suite of adaptations for an aquatic lifestyle and piscivorous diet that have previously been documented for *Spinosaurus*[7,13,14]. Although developed to a lesser degree, aquatic adaptations are also found in other members of the spinosaurid clade[15,16], which had a near-global distribution and a stratigraphic range of more than 50 million years[14], pointing to a substantial invasion of aquatic environments by dinosaurs.

Detailed anatomical and functional studies, combined with abundant trackways, all point to a strictly terrestrial ecology for dinosaurs[1], with one clade (Maniraptora) taking to the air[17]. Dinosaurs are not currently thought to have invaded aquatic environments, following the abandonment—several decades ago[5,6]—of century-old ideas of semi-aquatic habits in sauropods and hadrosaurs[2,3]. Potential semi-aquatic lifestyles have recently been hypothesized for a small number of dinosaurs[18,19]. However, the only group of dinosaurs for which multiple plausible lines of evidence indicate aquatic adaptations are the spinosaurids, large-bodied theropods interpreted as near-shore waders that fed on fish along the margins of (rather than within) bodies of water[10,15,20].

A recent study[7] of the largest known spinosaurid, *S. aegyptiacus*, identified a series of adaptations consistent with a semi-aquatic lifestyle, including reduced hindlimbs, wide feet with large flat unguals, long bones with a highly reduced medullary cavity, and a suite of cranial features (such as retracted nares, interlocking conical teeth and a rostromandibular integumentary sensory system). This interpretation has been challenged on the basis of taphonomy[9], biomechanical modelling[10] and anatomical concerns[9]. Locomotion in water is a major point of contention[10,11], because no unambiguous evidence for a plausible mode of propulsion has been presented. Furthermore, our understanding of the anatomy and ecology of this highly derived theropod has been hampered because only one associated *Spinosaurus* skeleton exists, with all other associated remains having been destroyed in World War II[7]. The posterior portion of the skeleton and the caudal vertebral series in particular, which has the potential to shed light on likely adaptations for aquatic locomotion, has until now been poorly understood[12]. Consequently, the tail anatomy and function of *Spinosaurus* has been reconstructed on the basis of highly incomplete remains and potentially spurious comparisons with other similar-sized theropods.

[1]Department of Biology, University of Detroit Mercy, Detroit, MI, USA. [2]Associazione Paleontologica Paleoartistica Italiana, Parma, Italy. [3]Sezione di Paleontologia dei Vertebrati, Museo di Storia Naturale di Milano, Milan, Italy. [4]Department of Geology and Geophysics, Yale University, New Haven, CT, USA. [5]Dipartimento di Scienze della Terra 'A. Desio', Università degli Studi di Milano, Milan, Italy. [6]School of the Environment, Geography and Geological Sciences, University of Portsmouth, Portsmouth, UK. [7]Department of Geology, Hassan II University of Casablanca, Casablanca, Morocco. [8]School of Museum Studies, University of Leicester, Leicester, UK. [9]Staatliches Naturhistorisches Museum Braunschweig, Braunschweig, Germany. [10]Museum of Comparative Zoology and Department of Organismic and Evolutionary Biology, Harvard University, Cambridge, MA, USA. ✉e-mail: ibrahini@udmercy.edu; spierce@oeb.harvard.edu

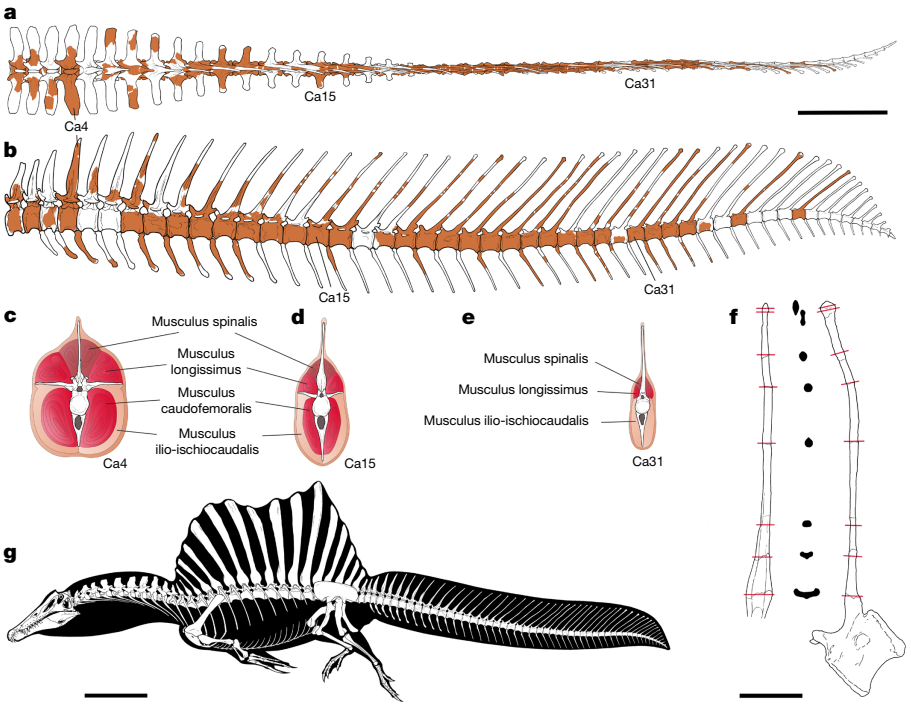


**Fig. 1 | Reconstructed skeleton and caudal series of FSAC-KK 11888.** **a**, **b**, Caudal series (preserved parts shown in colour) in dorsal view (**a**) and left lateral view (**b**). **c**–**e**, Reconstructed sequential cross-sections through the tail show proximal-to-distal changes in the arrangement of major muscles. **f**, Sequential cross-sections through the neural spine of caudal vertebra 23 (Ca23) to show apicobasal changes. **g**, Skeletal reconstruction. Scale bars, 50 cm (**a**–**e**), 10 cm (**f**), 1 m (**g**).

Here we describe a nearly complete and partially articulated tail of a subadult individual of *S. aegyptiacus* (accession code Faculté des Sciences of Casablanca University (FSAC)-KK 11888), from the Cretaceous Kem Kem beds of south-eastern Morocco (Figs. 1, 2, Extended Data Figs. 1–4, Supplementary Information section 1, Supplementary Video 1). The skeleton represents, to our knowledge, the most complete dinosaur known from the Kem Kem beds[21,22] and the most complete skeleton of a Cretaceous theropod known from mainland Africa (Supplementary Information section 2). As we show here, the tail forms part of the neotype of *S. aegyptiacus*[7] and was found in direct juxtaposition to the remainder of the skeleton (Extended Data Fig. 3). The newly recovered material confirms the previous conclusion[7] that a single subadult individual is preserved at the site; over 90% of the new material was recovered during field excavations in late 2018, and then digitally recorded (Extended Data Figs. 1–4, Supplementary Information sections 2–5). Several elements conform closely to drawings of the *Spinosaurus* fossils that were destroyed in World War II (Extended Data Fig. 6).

More than 30 near-sequential caudal vertebrae (located within caudal positions 1–41) of FSAC-KK 11888 are preserved, and represent approximately 80% of the original tail length (Extended Data Figs. 3, 4, Extended Data Tables 1, 2). Both proximal and distal elements of the tail are complete and preserved in three dimensions, indicating minimal taphonomic distortion (Fig. 2, Supplementary Video 2). At the level of the caudal transition point[1], the centra become proportionally more elongate. In addition, the prezygapophyses no longer overhang the preceding centrum and show a marked decrease in size compared to those of many theropod dinosaurs[1]. The postzygapophyses also decrease in size (Fig. 2), leading to a reduced contact with the prezygapophyses, and are absent in the distalmost caudal vertebrae. This again is different from the condition seen in most theropods, in which zygapophyses become more elongate and more prominent towards the tail tip[1], restricting flexibility in more distal intervertebral joints.

The neural arches are distinctive elements of the *Spinosaurus* tail. A notably complex array of vertebral laminae and fossae is present in the proximal caudal vertebrae, and partly persists in mid-caudal neural arches. The morphology of the neural spines shows considerable variation along the sequence (Figs. 1, 2, Extended Data Table 1): the spines of the proximal caudal vertebrae are about three times taller than their centra and are cross-shaped in cross-section from their base to mid-height; in mid-caudal vertebrae, the spines become much longer; and in the small distal caudal vertebrae, the length of the neural spines reaches well over seven times the height of the centrum, in contrast to the condition suggested in a previous study[11]. The neural spines of mid-distal caudal vertebrae of *Spinosaurus* have a cross-section that is unique among theropods: they are proximodistally—rather than transversely—flattened. This is owing to the hyper-development of the spinodiapophyseal laminae and the loss of pre- and postspinal laminae. The chevrons also differ from those of other theropods. The morphology of the chevrons in *Spinosaurus* varies little throughout the caudal series, except for a slight gradual reduction of the haemal canal: distal chevrons are as elongate as the proximal chevrons (Extended Data Table 2) but become slender, paralleling the gradual decrease in the size of the centra. Taken together, the elongate neural and haemal arches result in a tail shape that is markedly vertically expanded and has an extensive lateral surface area (Fig. 1, Extended Data Figs. 3, 4).

The skeletal anatomy of *Spinosaurus* represents a major departure from that of other theropods—including from that of other members of the Tetanurae clade (which comprises crown group birds and all other stem theropods more closely related to birds than to *Ceratosaurus*[1]). One feature of the Tetanurae is a stiffened tail in which the degree of overlap in articulation between pre- and postzygapophyses increases along the caudal series, greatly diminishing the range of motion between individual vertebrae[1]. This trend toward reduced mobility is emphasized in paravians, with the appearance of ossified ligaments and/or reduction and fusion of the caudal vertebrae into a pygostyle[17]. By contrast, in *Spinosaurus* the pre- and postzygapophyses are much further reduced than in other tetanurans and—in the middle

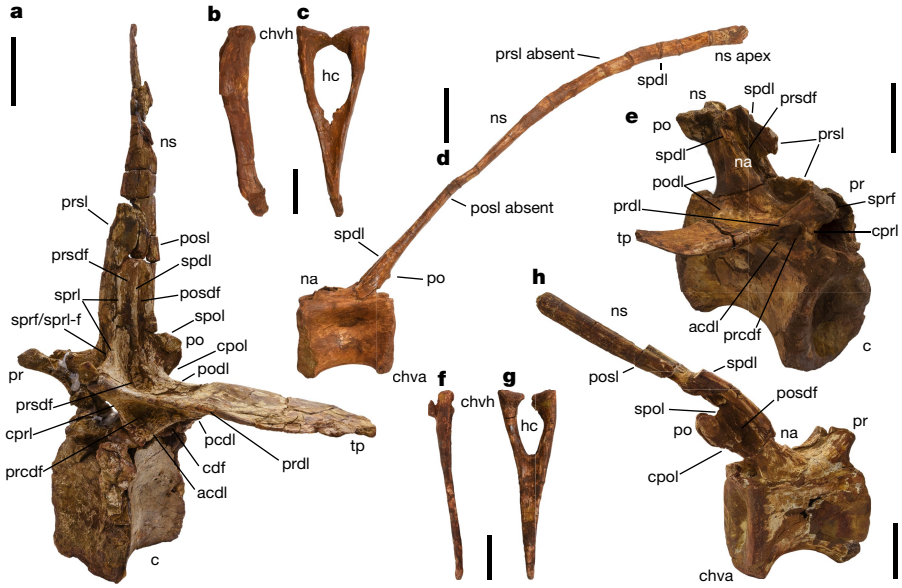


**Fig. 2 | Selected caudal vertebrae and chevrons of FSAC-KK 11888.** **a**, Proximal caudal vertebra (Ca4) in left proximolateral view. **b**, **c**, Proximal chevron (Chv7) in left lateral (**b**) and proximal (**c**) view. **d**, Distal caudal vertebra (Ca31) in left lateral view. **e**, Mid-caudal vertebra (Ca12) in right proximolateral view. **f**, **g**, Distal chevron (Chv27) in left lateral (**f**) and proximal (**g**) views. **h**, Mid-caudal vertebra (Ca16) in right distolateral view. acdl, anterior centrodiapophyseal lamina; c, centrum; ca, caudal vertebra; cdf, centrodiapophyseal fossa; chva, chevron articulation; chvh, chevron head; cpol, centropostzygapophyseal lamina; cprl, centroprezygapophyseal lamina; hc, haemal canal; na, neural arch; ns, neural spine; pcdl, posterior centrodiapophyseal lamina; po, postzygapophysis; pocdf, postzygapophyseal centrodiapophyseal fossa; podl, postzygodiapophyseal lamina; posdf, postzygapophyseal spinodiapophyseal fossa; posl, postspinal lamina; pr, prezygapophysis; prcdf, prezygapophyseal centrodiapophyseal fossa; prdl, prezygodiapophyseal lamina; prsdf, prezygapophyseal spinodiapophyseal fossa; prsl, prespinal lamina; spdl, spinodiapophyseal lamina; spol, spinopostzygapophyseal lamina; spof, spinopostzygapophyseal fossa; sprl, spinoprezygapophyseal lamina; sprl-f, spinoprezygapophyseal lamina fossa; tp, transverse process. Scale bars, 10 cm (**a**), 5 cm (**b**–**h**).

and distal portions of the tail—not only do not overlap, but almost disappear (Fig. 2); this allows the caudal region considerable flexibility, especially with regard to lateral movements.

We hypothesized that the highly specialized morphology of the *Spinosaurus* tail allowed it to function as a propulsive structure for aquatic locomotion. To test this idea, we evaluated the swimming potential of the *Spinosaurus* tail shape by comparing it to the tails of two terrestrial theropods (*Coelophysis bauri* and *Allosaurus fragilis*), two semi-aquatic tetrapods (the crocodile *Crocodylus niloticus* and the crested newt *Triturus dobrogicus*) and a rectangular control. Two-dimensional tail shapes were cut from 0.93-mm-thick plastic of flexural stiffness $5.8 \times 10^{-5}$ Nm$^2$. The plastic tails were attached to a robotic controller and actuated in a water flume to provide tail-tip amplitudes that were approximately 40% of tail length during swimming at 0.5 tail lengths per second. This swimming speed and amplitude of motion is similar to that of slow aquatic locomotion in modern tetrapods[23–25]. We measured swimming performance by quantifying the mean thrust and efficiency using a six-axis force–torque sensor attached to the shaft that drove each tail shape[26] (Fig. 3, Methods, Supplementary Fig. 4, Supplementary Videos 3–5).

Our experimental results show that the *Spinosaurus* tail shape was capable of generating more than 8 times the thrust of the tail shapes of other theropods, and achieved 2.6 times the efficiency (Fig. 3, Supplementary Data 1). The greatest thrust was achieved by the tail shape of the crested newt (1.8 times that of *Spinosaurus* and 14.8 times that of *Coelophysis*), but the crocodile tail shape achieved greater propulsive efficiency (1.5 times that of *Spinosaurus* and 4.0 times that of *Coelophysis*), comparable to the rectangular control (Fig. 3). The lower efficiency recovered in this experiment for *Spinosaurus* (compared to the control with the same surface area) and the crested newt indicates an effect of tail shape on performance. Overall, the vertically expanded tail shape of *Spinosaurus* imparts a substantial positive benefit to aquatic propulsion relative to the long and narrow tails of terrestrial theropods, supporting the inference that *Spinosaurus* used tail-propelled swimming. This tail morphology may have also increased the lateral stability of the body in the water, reducing the tendency to roll while floating[10].

Contrary to recent suggestions[10] that *Spinosaurus* was confined to wading and the apprehension of prey from around the edges of bodies of water, the morphology and function of its tail—along with its other adaptations for life in water[7]—point to *Spinosaurus* having been an active and highly specialized aquatic predator that pursued and caught its prey in the water column (Extended Data Fig. 7). The skeletal remains of *Spinosaurus* (Supplementary Information) from the Kem Kem beds—composed of sediments deposited in a major fluvio-deltaic system[7] that have yielded a diverse vertebrate assemblage[27]—provide further insights into the ecology of this dinosaur. The composition of the ecosystem represented by the Kem Kem assemblage is highly atypical, containing a rich freshwater fauna dominated by fishes (including lungfish and large-to-very-large sawfish and coelacanths[27]), a diverse range of crocodyliforms[28] and several giant predatory dinosaurs[7,22]. The seemingly anomalous occurrence in the same deposits of several large-bodied predators but few terrestrial herbivores is partially explained by the largely aquatic and probably piscivorous lifestyle of *Spinosaurus*, which considerably expands the morphological and ecological disparity of Kem Kem tetrapods[7,29]. At the same time, competition with several co-occurring large aquatic predators[28] may have driven the evolution of giant size in *Spinosaurus*.

Although the unique postcranial adaptations of *Spinosaurus* point towards an entirely novel mode of locomotion within Dinosauria, other spinosaurids share a wide range of derived anatomical features that are consistent with a partially aquatic, piscivorous mode of life[7,8,11,14,30]. The exact extent to which an aquatic lifestyle was adopted by these taxa, and how this varied across Spinosauridae, remains to be established. However, the near-global distribution of spinosaurids (which have now been reported from Europe, Asia, Africa and South America[30]) and their

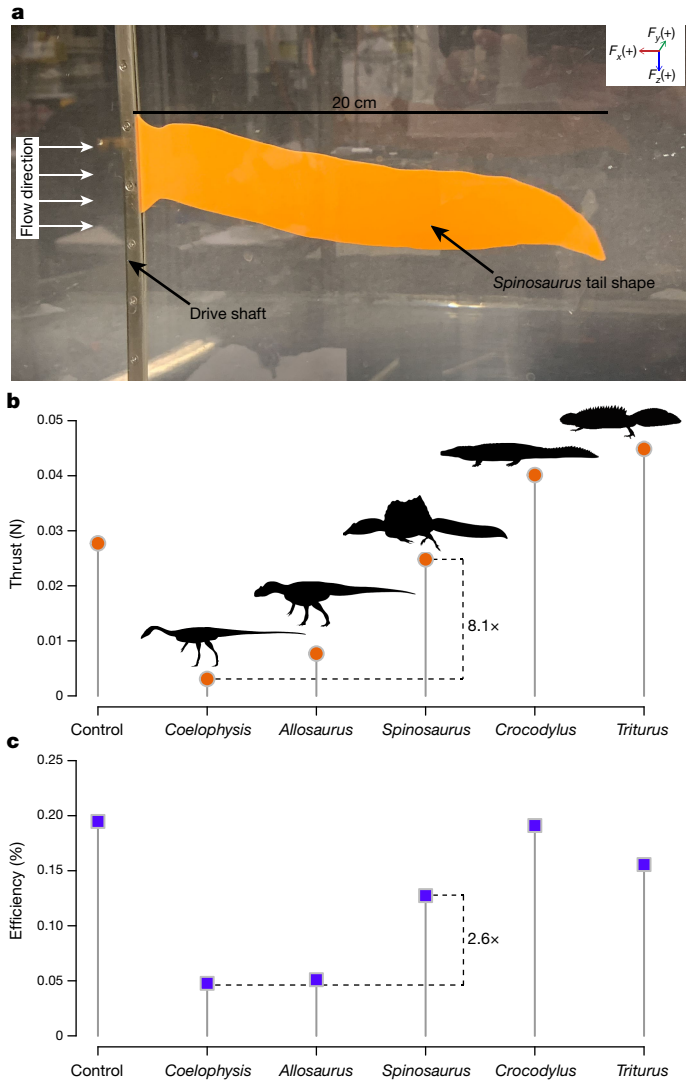


**Fig. 3 | Comparative tail swimming performance. a**, *Spinosaurus* plastic tail shape attached to a robotic drive shaft in a water flume with water flowing at 10 cm $s^{-1}$. With reference to the tail, positive *x* forces ($F_x$) are generated proximally (or upstream), positive *y* forces ($F_y$) in the right lateral direction, and positive *z* forces ($F_z$) in the ventral direction. **b**, **c**, Mean thrust (**b**) and mean efficiency (**c**) generated by tail shapes during robotically controlled swimming. All tails are scaled to 20-cm length (Supplementary Fig. 4). The control tail was rectangular in shape with the same surface area as the scaled *Spinosaurus* tail (63 $cm^2$). See Methods for experimental setup. Raw thrust and efficiency data, including mean and s.e.m., are provided in Supplementary Data 1. Swimming motions of the *Spinosaurus* tail are visualized in Supplementary Videos 3–5.

substantial temporal range (first appearing, based on phylogenetic inference, in the Mid—or possibly even Early—Jurassic epoch and with a fossil record that spans more than 50 million years (from the Late Jurassic to the early Late Cretaceous epoch)[14]) point to a persistent and widespread invasion of aquatic habitats by dinosaurs.

## Online content

Any methods, additional references, Nature Research reporting summaries, source data, extended data, supplementary information, acknowledgements, peer review information; details of author contributions and competing interests; and statements of data and code availability are available at https://doi.org/10.1038/s41586-020-2190-3.


1. Weishampel, D. B., Dodson, P. & Osmólska, H. *The Dinosauria* 2nd edn (Univ. of California Press, Berkeley, 2004).
2. Owen, R. A description of a portion of the skeleton of the *Cetiosaurus*, a gigantic extinct saurian reptile occurring in the oolitic formations of different portions of England. *Proc. Geol. Soc. Lond.* **3**, 457–462 (1841).
3. Cope, E. On the characters of the skull in the Hadrosauridae. *Proc. Acad. Nat. Sci. Philadelphia* **35**, 97–107 (1883).
4. Kermack, K. A. A note on the habits of sauropods. *Ann. Mag. Nat. Hist.* **4**, 830–832 (1951).
5. Bakker, R. T. Ecology of the brontosaurs. *Nature* **229**, 172–174 (1971).
6. Alexander, R. M. Mechanics of posture and gait of some large dinosaurs. *Zool. J. Linn. Soc.* **83**, 1–25 (1985).
7. Ibrahim, N. et al. Semiaquatic adaptations in a giant predatory dinosaur. *Science* **345**, 1613–1616 (2014).
8. Aureliano, T. et al. Semi-aquatic adaptations in a spinosaur from the Lower Cretaceous of Brazil. *Cretac. Res.* **90**, 283–295 (2018).
9. Evers, S. W., Rauhut, O. W. M., Milner, A. C., McFeeters, B. & Allain, R. A reappraisal of the morphology and systematic position of the theropod dinosaur *Sigilmassasaurus* from the "middle" Cretaceous of Morocco. *PeerJ* **3**, e1323 (2015).
10. Henderson, D. M. A buoyancy, balance and stability challenge to the hypothesis of a semi-aquatic *Spinosaurus* Stromer, 1915 (Dinosauria: Theropoda). *PeerJ* **6**, e5409 (2018).
11. Hone, D. W. E. & Holtz, T. R. Jr. Comment on: Aquatic adaptation in the skull of carnivorous dinosaurs (Theropoda: Spinosauridae) and the evolution of aquatic habits in spinosaurids. 93: 275–284. *Cretac. Res.* https://doi.org/10.1016/j.cretres.2019.05.010 (2019).
12. Stromer, E. Ergebnisse der Forschungsreisen Prof. E. Stromers in den Wüsten Ägyptens. II. Wirbeltier-Reste der Baharîje -Stufe (unterstes Cenoman). 3. Das Original des Theropoden *Spinosaurus aegyptiacus* nov. gen., nov. spec. *Abh. Kgl. Bayer. Akad. Wiss. Math. Phys. Kl. München* **28**, 1–28 (1915).
13. Vullo, R. et al. Convergent evolution of jaws between spinosaurid dinosaurs and Pike Conger Eels. *Acta Palaeontol. Pol.* **61**, 825–829 (2016).
14. Arden, T. M. S., Klein, C. G., Zouhri, S. & Longrich, N. R. Aquatic adaptation in the skull of carnivorous dinosaurs (Theropoda: Spinosauridae) and the evolution of aquatic habits in *Spinosaurus*. *Cretac. Res.* **93**, 275–284 (2019).
15. Charig, A. J. & Milner, A. C. *Baryonyx walkeri*, a fish-eating dinosaur from the Wealden of Surrey. *Bull. Nat. Hist. Mus. Geol.* **53**, 11–70 (1997).
16. Sues, H. D., Frey, E., Martill, D. M. & Scott, D. M. *Irritator challengeri*, a spinosaurid (Dinosauria: Theropoda) from the Lower Cretaceous of Brazil. *J. Vert. Pal.* **22**, 535–547 (2002).
17. Witmer, L. M. in *Mesozoic Birds: Above the Heads of Dinosaurs* (eds Chiappe, L. M. & Witmer, L. M.) 3–30 (Univ. California Press, 2002).
18. Tereschenko, V. Adaptive features of protoceratopoids (Ornithischia, Neoceratopsia). *Paleontol. J.* **42**, 273–286 (2008).
19. Cau, A. et al. Synchrotron scanning reveals amphibious ecomorphology in a new clade of bird-like dinosaurs. *Nature* **552**, 395–399 (2017).
20. Sereno, P. C. et al. A long-snouted predatory dinosaur from Africa and the evolution of spinosaurids. *Science* **282**, 1298–1302 (1998).
21. Lavocat, R. Sur les dinosauriens du Continental Intercalaire des Kem-Kem de la Daour. In *Comptes rendus 19e Congrès Géologique International, Alger, 1952* 65–68 (Academie des Sciences de Paris, 1954).
22. Sereno, P. C. et al. Predatory dinosaurs from the Sahara and Late Cretaceous faunal differentiation. *Science* **272**, 986–991 (1996).
23. D'Août, K. & Aerts, P. Kinematic and swimming efficiency of steady swimming in adult axolotls (*Ambystoma mexicanum*). *J. Exp. Biol.* **200**, 1863–1871 (1997).
24. Fish, F. Kinematics of undulatory swimming in the American alligator. *Copeia* **1984**, 839–843 (1984).
25. Frolich, L. M. & Biewener, A. A. Kinematic and electromyographic analysis of the functional role of the body axis during terrestrial and aquatic locomotion in the salamander *Ambystoma tigrinum*. *J. Exp. Biol.* **162**, 107–130 (1992).
26. Lauder, G. V., Flammang, B. & Alben, S. Passive robotic models of propulsion by the bodies and caudal fins of fish. *Integr. Comp. Biol.* **52**, 576–587 (2012).
27. Cavin, L. et al. Vertebrate assemblages from the early Late Cretaceous of southeastern Morocco: an overview. *J. Afr. Earth Sci.* **57**, 391–412 (2010).
28. Meunier, L. M. V. & Larsson, H. C. E. Revision and phylogenetic affinities of *Elosuchus* (Crocodyliformes). *Zool. J. Linn. Soc.* **179**, 169–200 (2017).
29. Amiot, R. et al. Oxygen and carbon isotope compositions of middle Cretaceous vertebrates from North Africa and Brazil: ecological and environmental significance. *Palaeogeogr. Palaeoclimatol. Palaeoecol.* **297**, 439–451 (2010).
30. Hone, D. W. E. & Holtz, T. R. A century of spinosaurs. A review and revision of the Spinosauridae with comments on their ecology. *Acta Geol. Sin.* **91**, 1120–1132 (2017).

# Methods

No statistical methods were used to predetermine sample size. The experiments were not randomized and investigators were not blinded to allocation during experiments and outcome assessment.

### Excavation and reconstruction

The Cretaceous Kem Kem beds of Morocco crop out along an extensive escarpment, often located near the Moroccan–Algerian border[7]. After the accidental discovery and partial excavation by a local collector in 2008, part of a single skeleton (FSAC-KK 11888)—subsequently deposited at the Faculté des Sciences of Casablanca University—was recovered, published and designated as the neotype of *S. aegyptiacus*[7]. A multi-institutional collaborative project in the years 2015–2019, led by N.I., resulted in four joint expeditions to the neotype site. Detailed and careful exploration of the debris around the site, as well as a systematic and extended excavation of the unexposed portion of the fossiliferous layer of the Zrigat hill, led to the recovery of many additional elements of the neotype skeleton (Extended Data Figs. 1–5). A detailed description of the newly recovered material, as well as the geological context, is included in the Supplementary Information. The Supplementary Information also includes details of a full-body flesh reconstruction of *Spinosaurus* based on FSAC-KK 11888, as well as estimates of whole-body mass, segment masses, segment centres of mass and whole-body centre of mass (Supplementary Data 2). The position of the centre of mass in comparison to that in previously published analyses[7,10] can be found in Extended Data Fig. 8.

### Osteohistological analysis

The aim of the osteohistological analysis was to determine whether the remains that were assigned to FSAC-KK 11888 belong to a single individual, rather than a chimeric association of juvenile and adult individuals preserved in the same location and at the same horizon. The analysis was based on five skeletal elements. The primary assumption is that, should histological details suggest that all five elements represent the same ontogenetic stage, then the remains are more likely to represent one individual than multiple individuals. By contrast, should these elements exhibit two or more distinct ontogenetic stages, this would point to the presence of multiple individuals of one taxon (or perhaps several taxa), all fortuitously preserved at a single location during a single depositional event[31–33].

The following elements were sectioned: the right femur; the left fibula; one rib; and two neural spines. All specimens were sectioned before preparation to ensure that no outer layers of the compact cortex were accidentally removed. In the case of the neural spines, the apical portion was sectioned.

Thin sectioning followed standard protocols[34]. The thin sections have a thickness of 50–70 µm, and were analysed with a petrographic microscope (Leica DM 2500 P). Digital images were captured using a ProgRes Cfscan camera. Only continuous lines were counted as lines of arrested growth. Annuli were interpreted as a single year, following a previous publication[35]. Retrocalculation, following a previously published method[36], was applied to determine the likely number of missing lines of arrested growth, eroded through remodelling of the bone. In the case of the neural spines, only the width of the innermost zone was used to retrocalculate the missing lines of arrested growth, because the shape of the section could not be approximated to a circular outline. The calculation of the major and minor axes used for the retrocalculation was performed in ImageJ[37]. Results of the histological analysis are included in the Supplementary Information.

### Experimental testing of tail-shape swimming performance

To test the aquatic locomotor potential of the newly reconstructed *S. aegyptiacus* tail, we determined the swimming performance of its tail shape using a robotic controller developed for studies of propulsive hydrodynamics[38–42]. The swimming performance of the *Spinosaurus* tail shape was compared to the performance of five other tail shapes from the following species: the small-bodied terrestrial theropod *C. bauri*, the large-bodied terrestrial theropod *A. fragilis*, the semi-aquatic crocodile *C. niloticus*, the semi-aquatic crested newt *T. dobrogicus* and a rectangular control tail that was scaled to the same surface area as the *Spinosaurus* tail. Tail shapes (Supplementary Fig. 4) were all scaled to 20 cm proximodistal length, manufactured from 0.93-mm-thick plastic of flexural stiffness $5.8 \times 10^{-5}$ Nm$^2$ and cut using an Epilog Zing 24 laser cutter.

The plastic tails were attached to a robotic controller that allowed us to impose specific motion programmes on the rigid shaft to which each tail was affixed (Fig. 3, Supplementary Videos 3–5). This shaft was moved in both heave (side-to-side) motion, as well as in pitch (angular rotation), to achieve undulatory tail motions. The imposed motion programme was 1-Hz frequency, ±1-cm heave and ±25° pitch, which resulted in the tail tip undergoing peak-to-peak lateral excursions of approximately 40% of the proximodistal length, comparable to that exhibited by swimming axolotls and alligators[23–25].

The shaft supporting each simulated tail at the leading edge was attached to an ATI (Apex) Nano-17 six-axis force–torque sensor located just above the water surface. Testing occurred in a recirculating water flume, and a free-stream flow of 0.5 l (10 cm s$^{-1}$) was imposed for all tests. Custom LabVIEW programs (National Instruments) were used to control flapping frequency, flow speed, heave and pitch. A custom LabVIEW program also was used to acquire data from the ATI transducer at a sampling rate of 1,000 Hz. Each tail shape was tested $n = 5$ times (except for the *Spinosaurus* tail, which was tested $n = 5$ times on 2 different days for a total of $n = 10$ tests). Output data can be found in Supplementary Data 1.

Thrust and efficiency for each tail shape were calculated using standard fluid dynamic equations as in previous research[43,44]. Mean thrust force ($F_x$) is calculated directly from transducer output from the $F_x$ channel, and we accounted for transducer rotation resulting from the pitch motion to provide the force component directed upstream (positive thrust). Propulsive efficiency is calculated as the ratio of the thrust coefficient ($C_T = 2\bar{F}x/\rho U^2 cs$) to the power coefficient ($C_p = 2\bar{P}/\rho U^3 cs$), in which $\rho$ is the fluid density, $U$ is the swimming velocity, $c$ is the foil chord and $s$ is the tail span. Effectively, this metric assesses the extent to which input power is translated into thrust.

### Reporting summary

Further information on research design is available in the Nature Research Reporting Summary linked to this paper.

## Data availability

The authors declare that all data supporting the findings of this study are available in the paper and its Supplementary Information. Three-dimensional data are available on SketchFab: flesh model at https://sketchfab.com/3d-models/07b2b6bf4c464c09bd30daa629f266ff; scanned caudal vertebrae and chevrons at https://sketchfab.com/3d-models/chv-7-ca70592e5d07408980220d639bc1456f (Chv7), https://sketchfab.com/3d-models/chv-24-d917f541a7934492aaf0be7c5b97ad40 (Chv24), https://sketchfab.com/3d-models/ca-4-56e19d32f53043369ba23d5283279eef (Ca4), https://sketchfab.com/3d-models/ca-7-c2f551b61e294138954c4f2224bd3353 (Ca7), https://sketchfab.com/3d-models/ca-12-bb2f30fec9064645b2ff99be30f1ac92 (Ca12), https://sketchfab.com/3d-models/ca-16-3cd5f6713e1f43f5bf466471416f06c8 (Ca16), https://sketchfab.com/3d-models/ca-23-f34b71eaf4e54cb29a89a0f50730e70a (Ca23), https://sketchfab.com/3d-models/ca-24-4e21ecea81c8403484b9b7e3da7bd0d6 (Ca24), https://sketchfab.com/3d-models/ca-31-6d0748a851994d6d86b84803743b75a4 (Ca31) and https://sketchfab.com/3d-models/ca-41-34e5e6415f7d4fcea335e7120b9fe9b4 (Ca41).

31. Ryan, M. J., Russell, A. P., Eberth, D. A. & Currie, P. J. The taphonomy of a *Centrosaurus* (Ornithischia: Ceratopsidae) bone bed from the Dinosaur Park Formation (Upper Campanian), Alberta, Canada, with comments on cranial ontogeny. *Palaios* **16**, 482–506 (2001).
32. Erickson, G. M., Currie, P. J., Inouye, B. D. & Winn, A. A. Tyrannosaur life tables: an example of nonavian dinosaur population biology. *Science* **313**, 213–217 (2006).
33. Bertozzo, F., Dalla Vecchia, F. M. & Fabbri, M. The Venice specimen of *Ouranosaurus nigeriensis* (Dinosauria, Ornithopoda). *PeerJ* **5**, e3403 (2017).
34. Chinsamy, A. & Raath, M. A. Preparation of fossil bone for histological examination. *Palaeontol. Afr.* **29**, 39–44 (1992).
35. Lee, A. H. & O'Connor, P. M. Bone histology confirms determinate growth and small body size in the noasaurid theropod *Masiakasaurus knopfleri*. *J. Vertebr. Paleontol.* **33**, 865–876 (2013).
36. Horner, J. R. & Padian, K. Age and growth dynamics of *Tyrannosaurus rex*. *Proc. R. Soc. Lond. B* **271**, 1875–1880 (2004).
37. Schneider, C. A., Rasband, W. S. & Eliceiri, K. W. NIH Image to ImageJ: 25 years of image analysis. *Nat. Methods* **9**, 671–675 (2012).
38. Lauder, G. V., Anderson, E. J., Tangorra, J. & Madden, P. G. A. Fish biorobotics: kinematics and hydrodynamics of self-propulsion. *J. Exp. Biol.* **210**, 2767–2780 (2007).
39. Lauder, G. V. et al. Robotic models for studying undulatory locomotion in fishes. *Mar. Technol. Soc. J.* **45**, 41–55 (2011).
40. Quinn, D. B., Lauder, G. V. & Smits, A. J. Maximizing the efficiency of a flexible propulsor using experimental optimization. *J. Fluid Mech.* **767**, 430–448 (2015).
41. Rosic, M. N., Thornycroft, P. J. M., Feilich, K. L., Lucas, K. N. & Lauder, G. V. Performance variation due to stiffness in a tuna-inspired flexible foil model. *Bioinspir. Biomim.* **12**, 016011 (2017).
42. Saadat, M. et al. On the rules for aquatic locomotion. *Phys. Rev. Fluids* **2**, 083102 (2017).
43. Read, D. A., Hover, F. S. & Triantafyllou, M. S. Forces on oscillating foils for propulsion and maneuvering. *J. Fluids Structures* **17**, 163–183 (2003).
44. Shelton, R. M., Thornycroft, P. J. & Lauder, G. V. Undulatory locomotion of flexible foils as biomimetic models for understanding fish propulsion. *J. Exp. Biol.* **217**, 2110–2120 (2014).



**Acknowledgements** We thank M. Azroal, H. Azroal, M. Fouadassi and all other expedition members from the 2015, 2018 and 2019 seasons for assistance in the field; A. A. Ha for help in preparing the fossils; the Moroccan Ministry of Mines, Energy and Sustainable Development for providing fieldwork permits; F. Manucci for helpful discussions about the flesh reconstruction of *Spinosaurus*; and P. Fahn-Lai for coding assistance. This research was supported by a National Geographic Society grant to N.I. (CP-143R-170), a National Geographic Emerging Explorer Grant to N.I., contributions from the Board of Advisors of the University of Detroit Mercy to N.I., a Jurassic Foundation grant to M.F., a Paleontological Society grant to M.F., an Explorers Club grant to M.F., as well as financial support from the Lokschuppen Rosenheim, the Museo di Storia Naturale di Milano, J. Pfauntsch and A. Lania.


**Author contributions** N.I. led the expeditions and the project. N.I., S.M., C.D.S., M.F., M.A., D.M.M., G.B., S.Z., D.A.M. and A.A. collected the specimens in the field. N.I., S.M., C.D.S., M.F., J.W., G.V.L. and S.E.P. designed the research. N.I., S.M., C.D.S., M.F., J.W., G.V.L. and S.E.P. designed and performed the experiments. N.I., S.M., C.D.S., M.F., M.A., D.M.M., J.W., G.B., S.Z., D.A.M., D.M.U., U.J., J.J., A.A., G.V.L. and S.E.P. analysed the data. G.B., M.A., C.D.S., S.E.P., D.M.M., S.M., M.F. and D.B. created the figures. D.B. sculpted the life reconstruction. N.I., S.M., C.D.S., M.F., J.W., D.M.U., G.V.L. and S.E.P. wrote the manuscript, which was reviewed by all authors.

**Competing interests** The authors declare no competing interests.

**Additional information**


**Supplementary information** is available for this paper at https://doi.org/10.1038/s41586-020-2190-3.



**Correspondence and requests for materials** should be addressed to N.I. or S.E.P.



**Peer review information** *Nature* thanks Matthew C. Lamanna, John A. Nyakatura and the other, anonymous, reviewer(s) for their contribution to the peer review of this work.

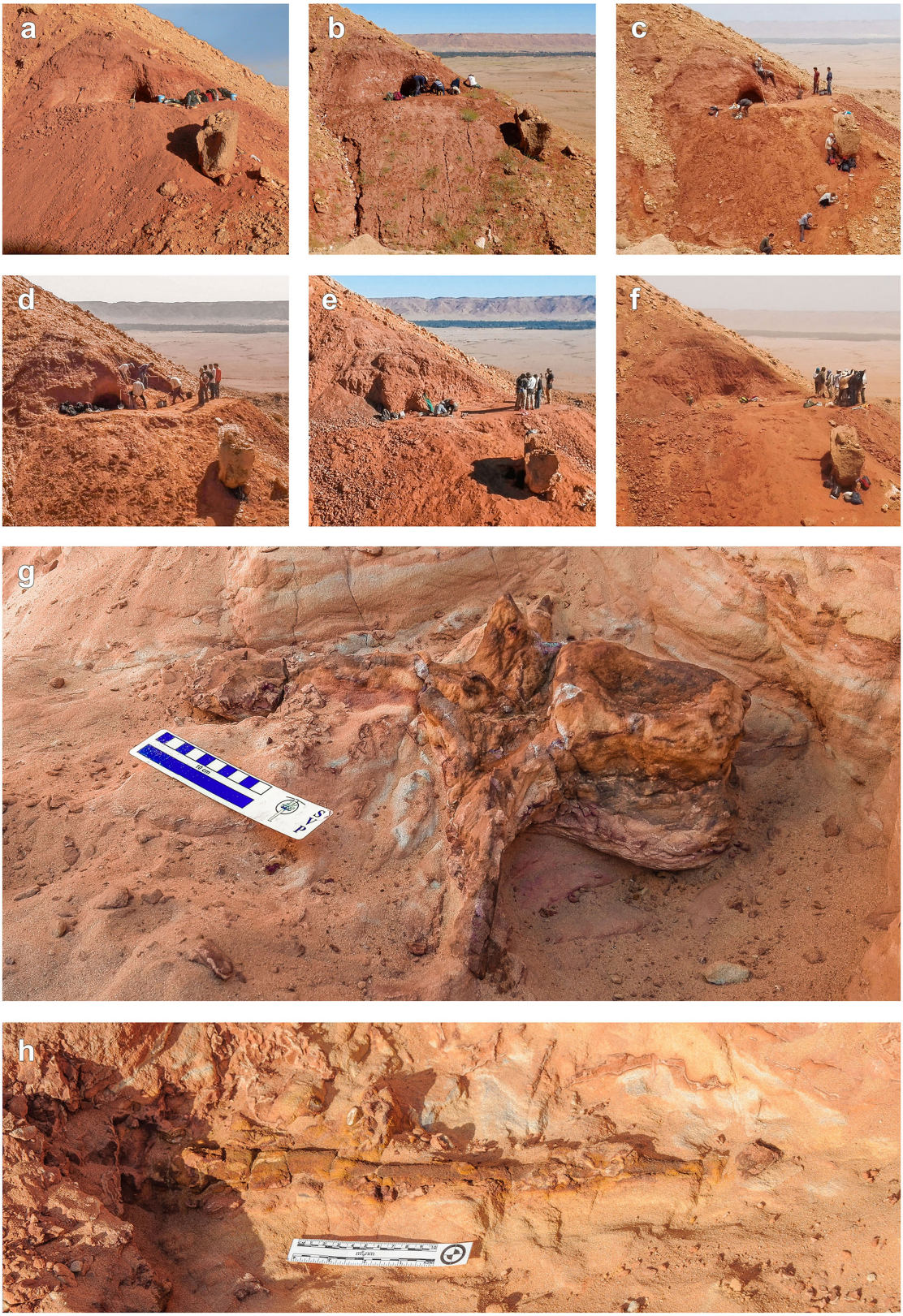


**Extended Data Fig. 1 | Excavation of the FSAC-KK 11888 site. a**–**f**, Different stages of the excavation, which resulted in the removal of over 15 tons of rock using a range of tools, including picks, brushes, hammers and a jackhammer. **a**, 17 November 2013. **b**, 29 March 2015. **c**, 17 September 2018. **d**, 19 September 2018. **e**, 5 December 2018. **f**, 21 July 2019. **g**, **h**, Selected bones in situ. **g**, Largely complete proximal caudal vertebra (Ca4). **h**, Neural spine of a mid-distal caudal vertebra, fragmented by syndiagenetic cracks. Scale bars, 10 cm.

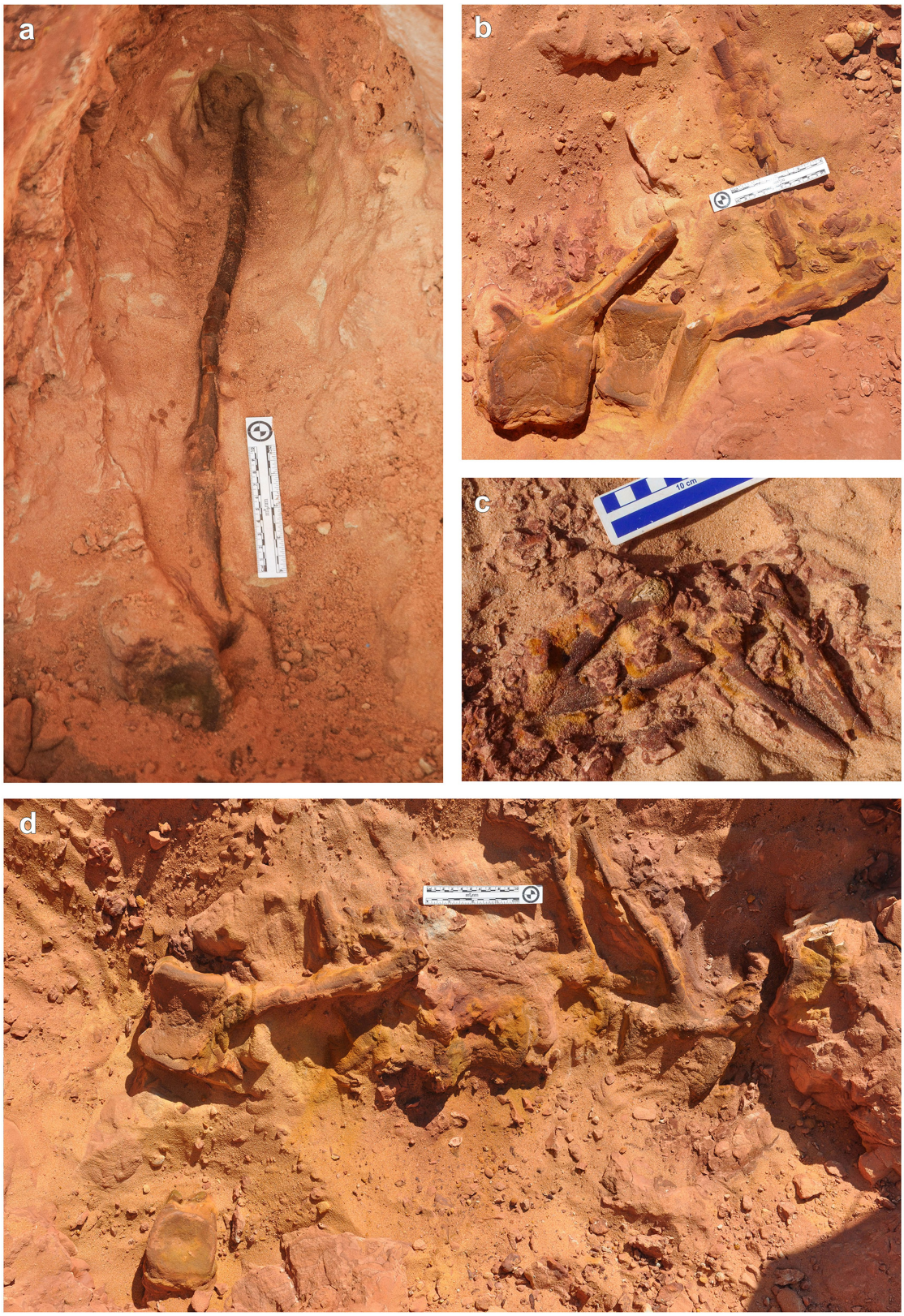


**Extended Data Fig. 2 | Excavation of the caudal elements of FSAC-KK 11888.** **a**, Largely complete distal caudal vertebra (Ca31), recovered in its entirety by digging a tunnel until the apex of the neural spine was reached. **b**, Semi-articulated mid-caudal vertebrae. **c**, Two haemal arches. **d**, Close association of middle caudal elements. Scale bars, 10 cm.

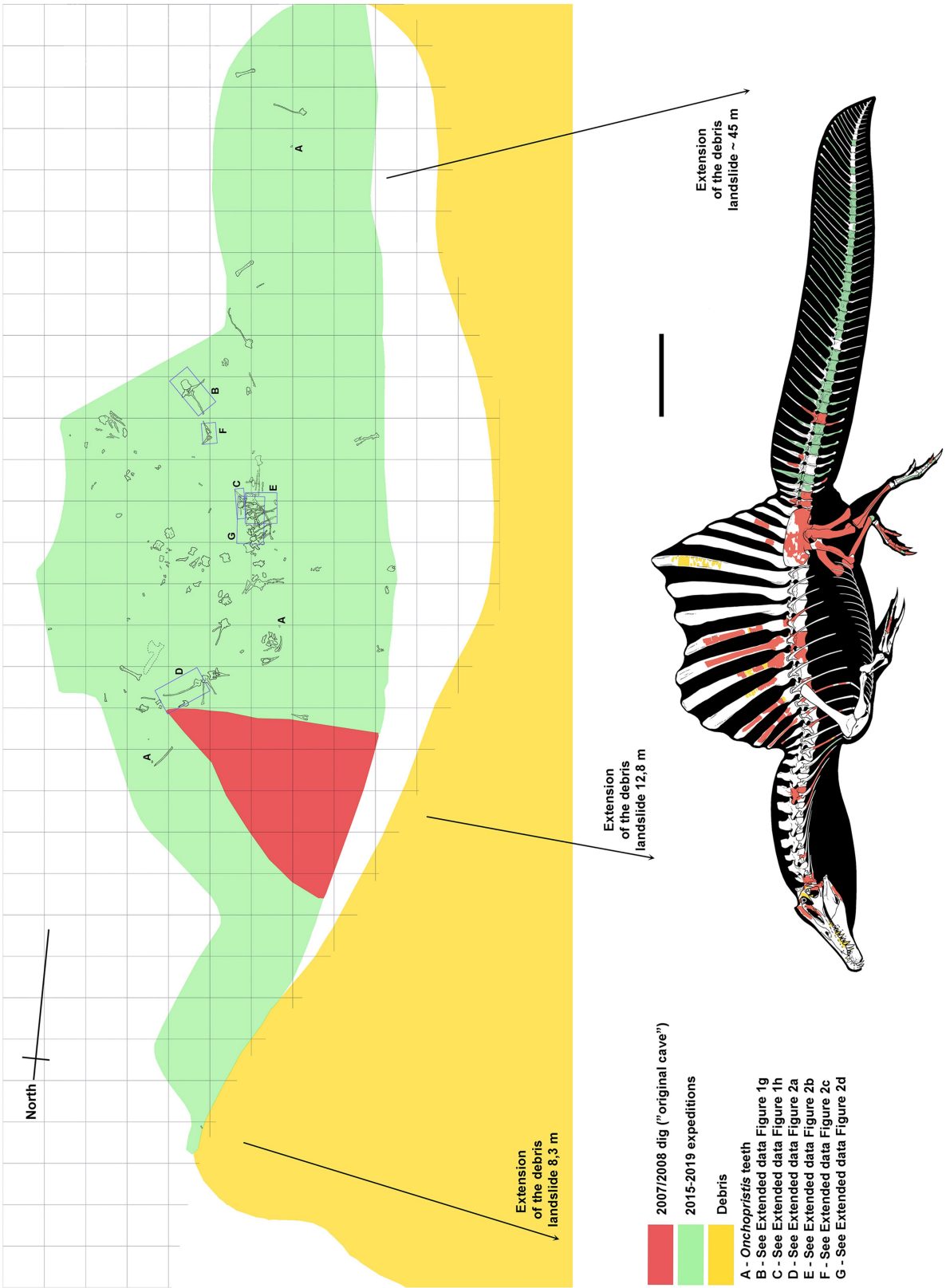


**Extended Data Fig. 3 | Excavation map and skeletal reconstruction.** Detailed map of the site of discovery of FSAC-KK 11888, and fully revised skeletal reconstruction. Colours in the map and reconstruction correspond to different phases of excavation: the local discovery in 2007–2008 (red), our excavations during the 2015–2019 expeditions (green) and sieving in the debris area during the 2015–2019 expeditions (yellow). Both images are at the same scale. Scale bar, 1 m.

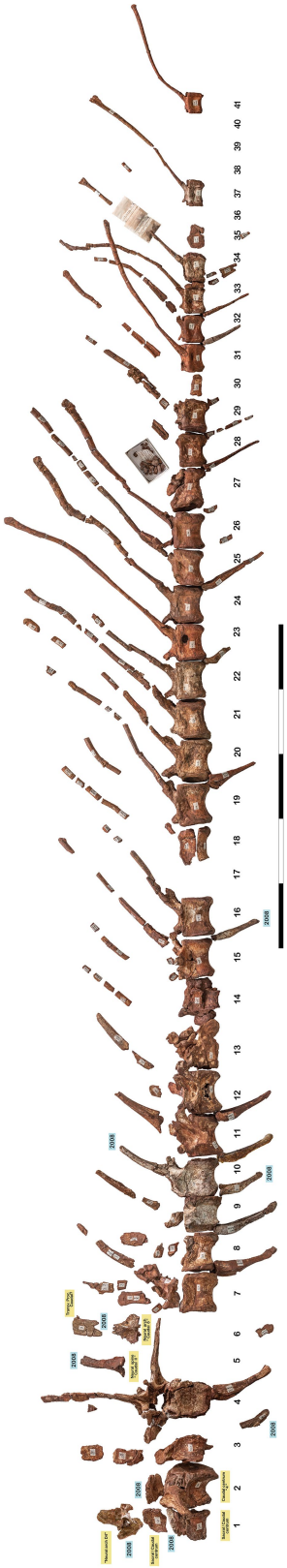

**Extended Data Fig. 4 | The caudal series of FSAC-KK 11888.** Photograph of the entire caudal series (numbered). Scale bar, 1 m.


**Extended Data Fig. 5 | Elements of FSAC-KK 11888 from 2008 (first excavation) and 2019 (most recent excavation), matched. a**–**t**, Evidence of the perfect match between elements collected by the local discoverer of the site in 2007–2008 (**a**, **e**, **f**, **i**, **k**, **m**, **n**, **p**, **q**, **s**) and elements excavated in situ or recovered from the site debris during the 2015–2019 excavations (**b**–**d**, **g**, **h**, **j**, **l**, **o**, **r**, **t**). **a**, **b**, Right and left metatarsal II. **c**, Left penultimate phalanx of the fourth pedal digit (IV-4) that came to light within the typical matrix in which bones of the FSAC-KK 11888 were embedded. **d**, **e**, Two possible splenial fragments reconnected. **f**–**i**, Phalanx IV-4 prepared and compared to the contralateral element of the right pes in dorsal view, and rearticulated with its ungual. **j**–**m**, Two complementary (broken) halves of the left squamosal and of a dorsal rib. **n**–**p**, **s**, **t**, Two key fragments from the debris, reconnecting the base and the shaft of a neural spine (possibly the 7th). **q**, **r**, The right astragalus (excavated in situ in July 2019) rearticulated to its tibia (from 2008). Arrows point to recomposed fractures.

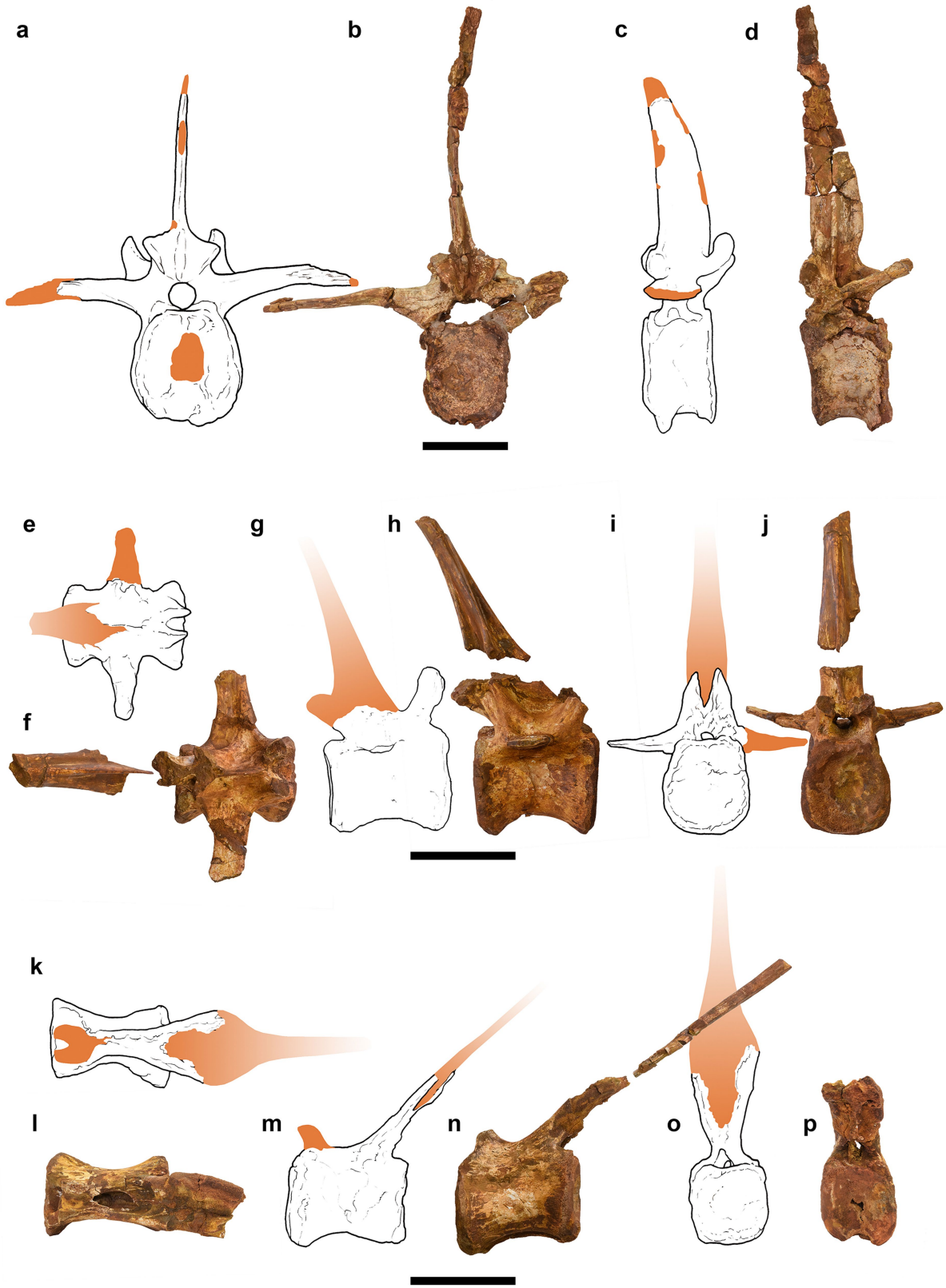


**Extended Data Fig. 6 | Comparison of FSAC-KK 11888 caudal vertebrae to those destroyed in World War II.** Comparison between the caudal vertebrae of the neotype of *S. aegyptiacus*, with those of the two specimens (the holotype and a specimen known as '*Spinosaurus* B', both of which are now lost) from the Bahariya Oasis (Egypt) described by E. Stromer[12]. **a**–**d**, Proximal caudal vertebra of the holotype (accession code BSP 1912 VIII 19) in distal (**a**) and right lateral (**c**) views; and of Ca4 of FSAC-KK 11888 in distal (**b**) and right lateral (**d**) views. **e**–**j**, Proximal caudal vertebra of *Spinosaurus* B in dorsal (**e**), right lateral (**g**) and proximal (**i**) views; Ca11 of FSAC-KK 11888 in dorsal (**f**), right lateral (**h**) and proximal (**j**) views. **k**–**p**, Middle caudal vertebra of *Spinosaurus* B in dorsal (**k**), left lateral (**m**) and distal (**o**) views; Ca21 of FSAC-KK 11888 in dorsal (**l**), left lateral (**n**) and distal (**p**) views. Scale bars = 10 cm.

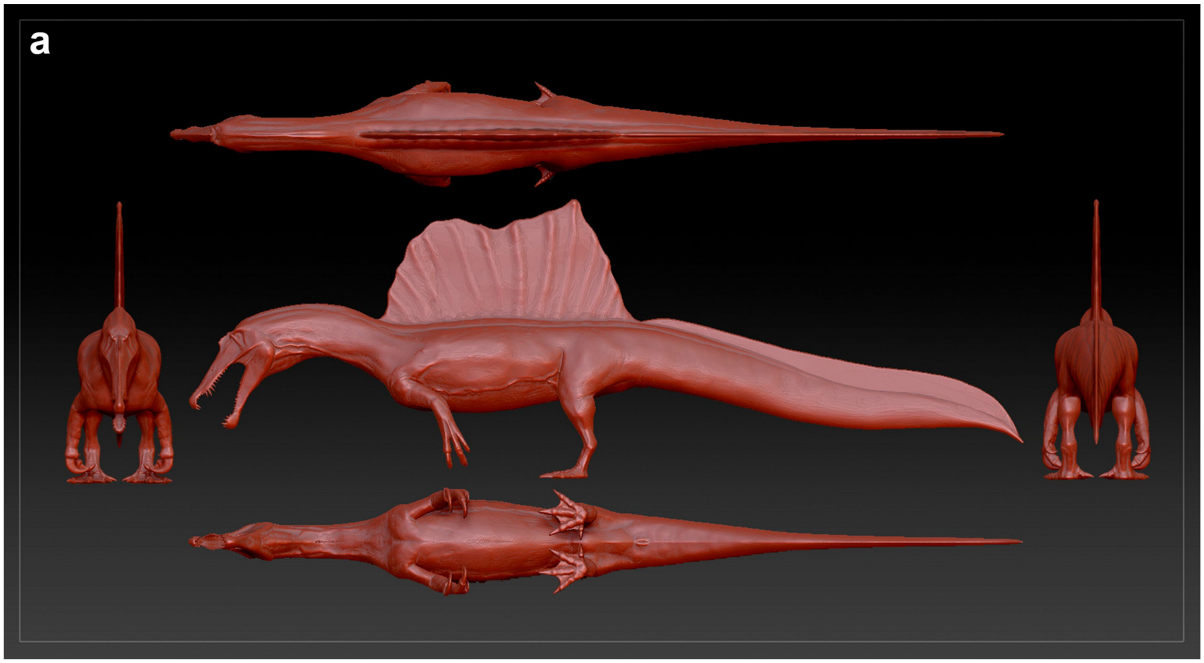


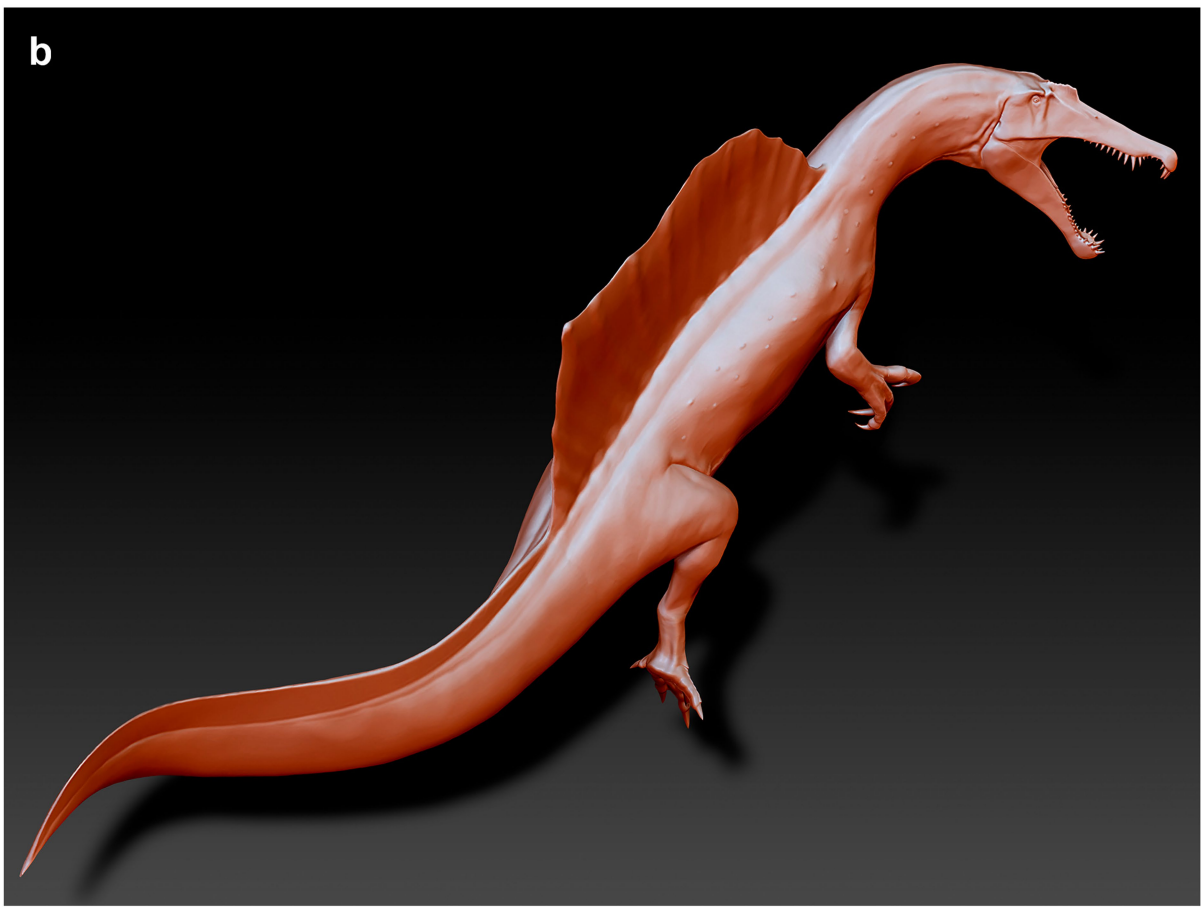


**Extended Data Fig. 7 | Three-dimensional fleshed-out model based on FSAC-KK 11888. a**, **b**, Symmetrical pose in five views (**a**) and swimming pose (**b**).

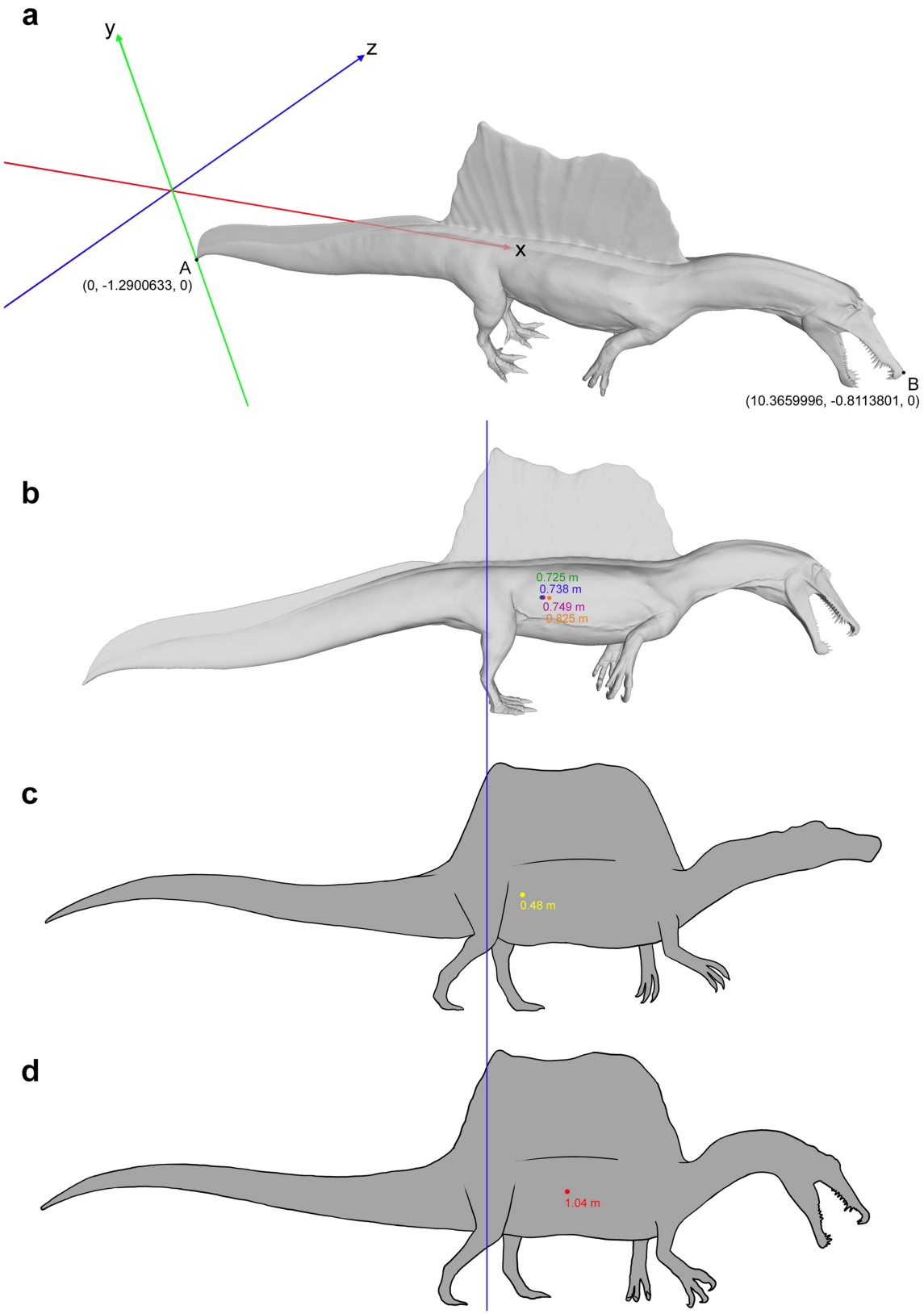


**Extended Data Fig. 8 | Whole-body centre of mass. a–d**, Snout tip and tail tip in the coordinate system (**a**) and centre-of-mass distance from the cranial margin of the acetabulum in this study (**b**), calculated using multiple approaches (Supplementary Information, Supplementary Data 2) and compared to the centre of mass in ref. [10] (**c**); and ref. [7] (**d**).

## Extended Data Table 1 | Measurements of caudal vertebrae of FSAC-KK 11888

| number in the series | proximodistal length of centrum | dorsoventral height proximal face of centrum | transverse diameter proximal face of centrum | minimum transverse diameter of centrum (constriction) | maximum length of neural spine (dorsal to the neural canal, along the curvature if any) | maximum width at transverse processes |
|---|---|---|---|---|---|---|
| **Ca1** | 78 | n.p. | n.p. | n.p. | 92 (p) | 320 (p, based on Ltp) |
| **Ca2** | 94 | 129 | 113 | 67 | n.p. | n.p. |
| **Ca3** | 75 (p) | n.p. | n.p. | n.p. | n.p. | n.p. |
| **Ca4** | 98 | 116 | 106 | 73 | 355 (p) | 480 (p, based on Ltp) |
| **Ca5** | n.p. | n.p. | n.p. | n.p. | 140 (p) | n.p. |
| **Ca6** | n.p. | n.p. | n.p. | n.p. | 59 (p) | n.p. |
| **Ca7** | 114 | 102 | 113 | 74 | 335 (p) | n.p. |
| **Ca8** | 112 | 97 | 108 | 64 | n.p. | n.p. |
| **Ca9** | 99 | 99 (e) | 81 (p) | 63 | n.p. | n.p. |
| **Ca10** | 115 (p, L)<br>106 (p, R) | 97 (e) | 76 (p, deformed) | 47 | 240 (p) | n.p. |
| **Ca11** | 113 | 91 | 86 | 49 | 180 (p) | 200 (p, almost complete) |
| **Ca12** | 122 | 101 | 75 | 41 | 250 (p) | 210 (based on R) |
| **Ca13** | 106 (e) | 79 (e) | 59 (p) | 33 (p) | n.p. | n.p. |
| **Ca14** | 117 | 64 (p) | n.p. | n.p. | n.p. | n.p. |
| **Ca15** | 120 | 84 | 80 | 47 | 375 (p) | 186 (p, based on L) |
| **Ca16** | 116 | 87 | 78 | 44 | 285 (p) | 106 (p, based on L) |
| **Ca17** | n.p. | n.p. | n.p. | n.p. | 210 (p) | n.p. |
| **Ca18** | 102 (p) | n.p. | n.p. | n.p. | 145 (p) | n.p. |
| **Ca19** | 115 | 84 | 70 | 35 | 445 (p) | n.p. |
| **Ca20** | 104 | 107 | 71 | 32 | 405 (p) | n.a. |
| **Ca21** | 109 | 78 | 77 | 44 | 525 (p) | n.a. |
| **Ca22** | 110 | 80 | 74 | 46 | 285 (p) | n.a. |
| **Ca23** | 103 | 78 | 72 | 45 | 540 | n.a. |
| **Ca24** | 110 | 78 | 67 | 35 | 535 (p) | n.a. |
| **Ca25** | 101 | 74 | 81 | 51 | 550 (p) | n.a. |
| **Ca26** | 104 | 77 | 76 | 51 | 480 (p) | n.a. |
| **Ca27** | 106 | 92 | 66 | 42 | n.p. | n.a. |
| **Ca28** | 102 | 71 | 65 | 32 (p, compressed) | n.p. | n.a. |
| **Ca29** | 90 | 70 | 71 | 36 (p, slightly collapsed) | 290 (p) | n.a. |
| **Ca30** | 68 (p) | n.p. | n.p. | n.p. | 295 (p) | n.a. |
| **Ca31** | 86 | 64 | 58 | 35 | 535 | n.a. |
| **Ca32** | 85 | 60 | 58 | 29 | 325 (p) | n.a. |
| **Ca33** | 91 | 67 | 51 | 29 | 505 (p) | n.a. |
| **Ca34** | 87 | 60 | 62 | 31 | 290 (p) | n.a. |
| **Ca35** | 75 (p) | n.p. | n.p. | n.p. | n.p. | n.a. |
| **Ca36** | n.p. | n.p. | n.p. | n.p. | n.p. | n.a. |
| **Ca37** | 90 | 46 | 43 | 29 | 455 | n.a. |
| **Ca41** | 68 | 39 | 37 | 21 | 384 | n.a. |

Measurements are in mm. (p), not complete, measured as preserved; n.p., not preserved; n.a., not applicable; e, estimated.

## Extended Data Table 2 | Measurements of chevrons of FSAC-KK 11888

| number in the series | maximum height | height (measured perpendicular to the proximodistal axis of the tail) | base transverse width | height haemal canal |
|---|---|---|---|---|
| **Chv3** | 52 | n.p. | n.p. | n.p. |
| **Chv5** | 91 | n.p. | n.p. | n.p. |
| **Chv6** | 195 (p) | 170 (p) | 72 | 74 |
| **Chv7** | 215 | 185 | 80 | 72 |
| **Chv8** | 204 | 160 | 73 | 73 |
| **Chv9** | 150 (p) | 130 (p) | n.p. | n.p. |
| **Chv11** | 195 | 170 | 81 | 73 |
| **Chv12** | 155 (p) | 143 (p) | n.p. | n.p. |
| **Chv19** | 160 (p) | 125 (p) | 72 | 64 |
| **Chv22** | 103 (p) | 90 (p) | n.p. | n.p. |
| **Chv24** | 224 | 205 | 65 | 65 |
| **Chv25** | 44 (p) | n.p. | n.p. | n.p. |
| **Chv27** | 210 | 185 | 63 | 55 |
| **Chv28** | 155 (p) | n.p. | n.p. | n.p. |
| **Chv29** | n.p. | n.p. | n.p. | n.p. |
| **Chv31** | 144 (p) | 135 (p) | 62 | 60 |
| **Chv32** | 176 (p)<br>180 (e) | 160 | 53 | 53 |
| **Chv33** | 140 (p) | n.p. | n.p. | n.p. |
| **Chv34** | 33 (p) | n.p. | n.p. | n.p. |

Measurements are in mm. (p), not complete, measured as preserved; n.p., not preserved; e, estimated.

nature research

Corresponding author(s): Nizar Ibrahim
(reference number: 2019-06-09085E)

Last updated by author(s): Jan 30, 2020

# Reporting Summary

Nature Research wishes to improve the reproducibility of the work that we publish. This form provides structure for consistency and transparency in reporting. For further information on Nature Research policies, see Authors & Referees and the Editorial Policy Checklist.

## Statistics

For all statistical analyses, confirm that the following items are present in the figure legend, table legend, main text, or Methods section.

| n/a | Confirmed |
|---|---|
| ☐ | ☒ The exact sample size (*n*) for each experimental group/condition, given as a discrete number and unit of measurement |
| ☐ | ☒ A statement on whether measurements were taken from distinct samples or whether the same sample was measured repeatedly |
| ☒ | ☐ The statistical test(s) used AND whether they are one- or two-sided<br>*Only common tests should be described solely by name; describe more complex techniques in the Methods section.* |
| ☒ | ☐ A description of all covariates tested |
| ☒ | ☐ A description of any assumptions or corrections, such as tests of normality and adjustment for multiple comparisons |
| ☐ | ☒ A full description of the statistical parameters including central tendency (e.g. means) or other basic estimates (e.g. regression coefficient) AND variation (e.g. standard deviation) or associated estimates of uncertainty (e.g. confidence intervals) |
| ☒ | ☐ For null hypothesis testing, the test statistic (e.g. *F*, *t*, *r*) with confidence intervals, effect sizes, degrees of freedom and *P* value noted<br>*Give P values as exact values whenever suitable.* |
| ☒ | ☐ For Bayesian analysis, information on the choice of priors and Markov chain Monte Carlo settings |
| ☒ | ☐ For hierarchical and complex designs, identification of the appropriate level for tests and full reporting of outcomes |
| ☒ | ☐ Estimates of effect sizes (e.g. Cohen's *d*, Pearson's *r*), indicating how they were calculated |

*Our web collection on statistics for biologists contains articles on many of the points above.*

## Software and code

Policy information about availability of computer code

| | |
|---|---|
| Data collection | Custom LabVIEW programs (National Instruments Corp., Austin, TX, USA) for experimental testing of swimming performance. |
| Data analysis | Blender 2.79, ZBrush 4r7, and ClayTools 3D 2.0 for model rendering and sculpting; FlashPrint 3.26.0 to cut 3D model; Meshlab 2016.12 and Python 3.7 (through platform Anaconda) for calculation of the Centre of Mass; Meshroom 2019.1.0 for photogrammetry; custom LabVIEW 2013 programs (National Instruments Corp., Austin, TX, USA) for experimental testing of swimming performance; ImageJ 1.51w for retrocalculation of missing Lines of arrested Growth (histology). |

For manuscripts utilizing custom algorithms or software that are central to the research but not yet described in published literature, software must be made available to editors/reviewers. We strongly encourage code deposition in a community repository (e.g. GitHub). See the Nature Research guidelines for submitting code & software for further information.

## Data

Policy information about availability of data

All manuscripts must include a data availability statement. This statement should provide the following information, where applicable:

- Accession codes, unique identifiers, or web links for publicly available datasets
- A list of figures that have associated raw data
- A description of any restrictions on data availability

The authors declare that all data supporting the findings of this study are available within the paper and its Supplementary Information files (Source data).

# Field-specific reporting

Please select the one below that is the best fit for your research. If you are not sure, read the appropriate sections before making your selection.

☐ Life sciences ☐ Behavioural & social sciences ☒ Ecological, evolutionary & environmental sciences

For a reference copy of the document with all sections, see nature.com/documents/nr-reporting-summary-flat.pdf

# Ecological, evolutionary & environmental sciences study design

All studies must disclose on these points even when the disclosure is negative.

| | |
|---|---|
| Study description | We present the first unambiguous evidence for an aquatic propulsive structure in a dinosaur, the giant theropod Spinosaurus aegyptiacus. This dinosaur has a tail with an unexpected and unique shape consisting of extremely tall neural spines, and elongate chevrons forming a large, flexible, fin-like organ capable of extensive lateral excursion. Using a mechanical flapping apparatus to measure undulatory forces in physical tail models, we show that the tail shape of Spinosaurus produces far greater thrust and efficiency than the tail shapes of terrestrial dinosaurs, comparable to that of extant aquatic vertebrates that use vertically expanded tails to generate forward propulsion while swimming. This conclusion is consistent with a suite of adaptations for an aquatic lifestyle and a piscivorous diet in Spinosaurus, and with a persistent and significant invasion of aquatic environments by spinosaurid dinosaurs. |
| Research sample | A nearly complete, partially articulated fossil tail of a subadult individual of Spinosaurus aegyptiacus (FSAC-KK 11888), from the Cretaceous Kem Kem beds of south- eastern Morocco. Plastic tail shapes from the following species: Spinosaurus aegyptiacus, Coelophysis bauri, Allosaurus fragilis, Crocodylus niloticus, Triturus dobrogicus, and a rectangular control tail scaled to the same surface area as the Spinosaurus tail. |
| Sampling strategy | Systematic collection of a partial dinosaur skeleton (one individual). Tail shape experiments: Coelophysis and Allosaurus are well known taxa and reflect a basal theropod and large-bodied theropod respectively. The two extant aquatic tetrapods (salamander and crocodile) were chosen as they are known for utilizing tail-propelled swimming. |
| Data collection | N.I. led the expeditions and the project. N.I., S.M., C.D.S., M.F., M.A., D.M.M., G.B., S.Z. D.M. and A.A. collected the specimens in the field. N.I., S.M., C.D.S., M.F., J.W., G.V.L. and S.E.P. designed the research. N.I., S.M., C.D.S., M.F., J.W., G.V.L. and S.E.P. designed and performed the experiments. N.I., S.M., C.D.S., M.F., M.A., D.M.M., J.W., G.B., S.Z. D.M., D.M.U., U.J., J.J., A.A., G.V.L., and S.E.P. analysed the data. |
| Timing and spatial scale | 2018-2019; the specimen was collected from the Kem Kem beds, which crop out along the Moroccan-Algerian border for over 250 km. The fossil was collected from a well-defined field site (site map included in our submission) located near the town of Zrigat. |
| Data exclusions | No data were excluded |
| Reproducibility | The experiments were repeated over multiple days to ensure consistent measures. All repeats were successful. |
| Randomization | We did not use quantitative approaches that would require randomization. |
| Blinding | Our study (field: palaeontology) does not include experiments that would require blinding. |

Did the study involve field work? ☒ Yes ☐ No

## Field work, collection and transport

| | |
|---|---|
| Field conditions | Desert escarpment close to Moroccan Algerian border |
| Location | In- and ex-situ on the slopes of a south-east facing escarpment fringing the Aferdou Zrigat plateau (Tafilalt basin, Akrabou Formation, Kem Kem beds). See Supplemental Information. |
| Access and import/export | Permits for fieldwork were obtained from Ministère de l'Energie, des Mines, et de l'Environnement. Permits: 4581/DE/2019 (issued on 17/07/2019) and 4118/DE/2018/DG (issued on 06.06.2018). The work was performed in close collaboration with researchers in Morocco (FSAC, Casablanca). The specimens collected are deposited at the Departement de Géologie/Laboratoire de Biodiversité et Santé, Faculté des Sciences Aïn Chock, Hassan II University, Casablanca, Morocco. |
| Disturbance | No disturbance |

# Reporting for specific materials, systems and methods

We require information from authors about some types of materials, experimental systems and methods used in many studies. Here, indicate whether each material, system or method listed is relevant to your study. If you are not sure if a list item applies to your research, read the appropriate section before selecting a response.

## Materials & experimental systems

| n/a | Involved in the study |
|---|---|
| ☒ | ☐ Antibodies |
| ☒ | ☐ Eukaryotic cell lines |
| ☐ | ☒ Palaeontology |
| ☒ | ☐ Animals and other organisms |
| ☒ | ☐ Human research participants |
| ☒ | ☐ Clinical data |

## Methods

| n/a | Involved in the study |
|---|---|
| ☒ | ☐ ChIP-seq |
| ☒ | ☐ Flow cytometry |
| ☒ | ☐ MRI-based neuroimaging |

# Palaeontology

| | |
|---|---|
| Specimen provenance | Permits for fieldwork were obtained from Ministère de l'Energie, des Mines, et de l'Environnement. Permits: 4581/DE/2019 (issued on 17/07/2019) and 4118/DE/2018/DG (issued on 06.06.2018). The work was performed in close collaboration with researchers in Morocco (FSAC, Casablanca). The specimens collected are deposited at the Departement de Géologie/Laboratoire de Biodiversité et Santé, Faculté des Sciences Aïn Chock, Hassan II University, Casablanca, Morocco. |
| Specimen deposition | Laboratoire de Biodiversité et Santé, Faculté des Sciences Aïn Chock, Hassan II University, Casablanca, Morocco |
| Dating methods | No new dates are provided |

☒ Tick this box to confirm that the raw and calibrated dates are available in the paper or in Supplementary Information.